C. R. Chimie 16 (2013) 613–620

Contents lists available at SciVerse ScienceDirect

Comptes Rendus Chimie

www.sciencedirect.com

Full paper/Mémoire

New acridinium trifluoromethanesulfonate stacks induced in the presence of organotin(IV) complexes

Laurent Plasseraud *, Hélène Cattey

Institut de chimie moléculaire de l'université de Bourgogne (ICMUB), UMR CNRS 6302, UFR sciences et techniques, 9, avenue Alain-Savary, BP 47870, 21078 Dijon cedex, France

ARTICLE INFO

Article history:
Received 2 October 2012
Accepted after revision 4 December 2012
Available online 11 January 2013

Keywords:
Crystal engineering
Self-assembly
Nitrogen heterocycles
Stacking interactions
Hydrogen bonds
Tin

ABSTRACT

Three new crystalline architectures based on acridinium trifluoromethanesulfonate salts $[C_{13}H_{10}N]^+[CF_3SO_3]^-$ have been isolated as single crystals from the reaction of the dimeric hydroxo di-*n*-butylstannane trifluoromethanesulfonato complex $[n\text{-}Bu_2Sn(OH)(H_2O)(CF_3SO_3)]_2$ (**1**) with acridine ($C_{13}H_9N$, Acr), in dichloromethane at room temperature. When an equimolar mixture of anthracene ($C_{14}H_{10}$, Ant) and acridine is initially used, the crystallization of a sandwich-type arrangement occurs, leading to the intercalation of one molecule of anthracene between two acridium trifluoromethanesulfonate salt molecules. In the three X-ray structures reported, the crystal packing involves the contribution of hydrogen bonding and aromatic ring interactions, as well as short contacts of type O···(H)C, F···(H)C and F···F.

1. Introduction

In the past, several examples of organotin(IV) trifluoromethanesulfonate complexes have been synthesized and structurally characterized by single-crystal X-ray diffraction analysis. The most recent review in this research area was published by J. Beckmann in 2005 [1]. From a synthetic point of view, organotin(IV) trifluoromethanesulfonates are obtained either by reacting organotin oxide with trifluoromethanesulfonic acid (HO_3SCF_3, HOTf) [2], or alternatively organotin chloride ($R_{(4-x)}SnCl_x$) with silver(I) trifluoromethanesulfonate (AgO_3SCF_3, Ag(OTf)) [3]. The resulting solid-state reports highlight a large structural versatility for $F_3CSO_3^-$ which can be ionic or non-ionic, describing then various coordination modes to tin atoms: mono-, bi- and tridentate as well as terminal, *pseudo*-terminal, and bridging [4]. Furthermore, organotin(IV) trifluoromethanesulfonate complexes can be used as pre-catalysts or catalysts for several organic reactions, such as the Mukaiyama aldol reaction [5], the Robinson annulation [6], the acetylation of alcohols [7], the transesterification of dimethyl carbonate with phenol [8], and the direct synthesis of dimethyl carbonate from carbon dioxide and methanol [9].

Parallel to our investigations on carbon dioxide activation by organotin(IV) compounds [10], we previously reported the reaction of phenazine (Phz) and di-*n*-butyltin(IV) trifluoromethanesulfonato complexes affording phenazinium trifluoromethanesulfonate salts. In the solid state N(H)···O hydrogen bonding and π-π stacking interactions lead to the self-assembly of supramolecular edifices [4b,11]. Herein we report the application of this unusual crystal engineering method with acridine (Acr), and three new supramolecular architectures. They are based on acridinium stacks promoted by the dimeric hydroxo di-*n*-butylstannane trifluoromethanesulfonato complex $[n\text{-}Bu_2Sn(OH)(H_2O)(CF_3SO_3)]_2$ (**1**) (Scheme 1).

2. Experimental

2.1. Materials and instrumentation

Organic solvents, dichloromethane (*Carlo Erba*, 99.5% purity), toluene (*Acros*, 99.99%) and *n*-pentane (*Carlo Erba*,

* Corresponding author.
E-mail address: laurent.plasseraud@u-bourgogne.fr (L. Plasseraud).

1631-0748/$ – see front matter © 2012 Académie des sciences. Published by Elsevier Masson SAS. All rights reserved.
http://dx.doi.org/10.1016/j.crci.2012.12.006

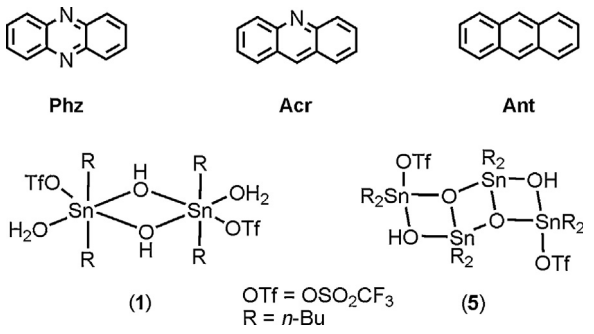

Scheme 1. Organic reactants and organotin(IV) compounds relating to this study.

99% purity) were refluxed over appropriate dessicants, distilled, and saturated with argon prior to use. Chemicals were purchased from *Acros Organics* and *Fluka*, and used without further purification. The starting compound [*n*-$Bu_2Sn(OH)(H_2O)(CF_3SO_3)]_2$ (**1**) was synthesized from *n*-Bu_2SnO (*Acros*, 98% purity) and trifluoromethanesulfonic acid (*Fluka*, 98% purity) according to a published method [2a]. The ^1H, ^{19}F, $^{119}Sn\{^1H\}$, and $^{13}C\{^1H\}$ NMR experiments were run at 298 K on a Bruker Avance 300 spectrometer (at the Plateforme d'Analyses Chimiques et de Synthèse Moléculaire de l'Université de Bourgogne – PACSMUB), at 300.131, 282.404, 111.910, and 75.475 MHz, respectively, and calibrated with Me_4Si, trifluoromethylbenzene or Me_4Sn as an internal standard. Chemical shift δ values are given in ppm. IR spectra were recorded on a Bruker Vector 22 equipped with a Specac Golden Gate™ ATR device. Melting points were determined in capillaries on an Electrothermal 9100 apparatus. Elemental analyses (C, H, N) were performed at the Institut de Chimie Moléculaire de l'Université de Bourgogne, Dijon.

2.2. Isolation of $[C_{13}H_{10}N{\cdot}H_2O][CF_3SO_3]$ (2) and $[C_{13}H_{10}N][CF_3SO_3]$ (3)

Three molar equivalents of acridine ($C_{13}H_9N$, *Acros*, 98% purity) (0.237 g, 1.322 mmol) were added to a colourless solution of [*n*-$Bu_2Sn(OH)(H_2O)(CF_3SO_3)]_2$ (**1**) (0.360 g, 0.441 mmol) in dichloromethane (15 mL) at room temperature. After stirring for two hours, fresh toluene (10 mL), used as co-solvent for crystallization, was then introduced to the resulting orange solution. After few days at room temperature, colourless single-crystals (squares and rods) were first obtained and attributed according to their IR fingerprints to oxo-cluster **5** which crystallized in fact in two polymorphic forms, **5a** (square) and **5b** (rod). After separation, two new types of coloured crystals, yellow needles and yellow squares, were grown from the mother-liquor by slow evaporation. The crystals were then filtered off, washed with portions of *n*-pentane, dried in air at room temperature, collected separately and finally characterized as salt **2** and **3**, respectively.

$[C_{13}H_{10}N{\cdot}H_2O][CF_3SO_3]$ (**2**) (mp 202 °C). ^1H NMR (CD_2Cl_2): δ 15.94 (brs, 1H, AcrH), 9.59 (s, 1H, AcrH), 8.70 (d, J = 8.9 Hz, 2H, AcrH), 8.38 (d, J = 8.5 Hz, 2H, AcrH), 8.30 (m, 2H, AcrH), 7.94 (m, 2H, AcrH), 1.56 (brs, 2H, H_2O). ^{19}F NMR (CD_2Cl_2): δ –78.97 (s, $CF_3SO_3^-$). $^{13}C\{^1H\}$ NMR (CD_2Cl_2): δ 148.5, 140.4, 138.4, 129.7, 128.8, 126.5, 121.0 (q, $^1J_{C\text{-}F}$ = 319 Hz, $CF_3SO_3^-$), 120.8. Anal. Calc. For $C_{14}H_{12}F_3NO_4S$ (347.31): C, 48.41; H, 3.48; N, 4.03. Found: C, 48.30; H, 3.29; N, 4.30%. Main IR bands (ν, cm^{-1}): 3387, 3088, 3048, 2522, 2052, 1643, 1486, 1467, 1402, 1382, 1321, 1246, 1224, 1166, 1152, 1143, 1025, 902, 862, 825, 778, 743, 675.

$[C_{13}H_{10}N][CF_3SO_3]$ (**3**) (mp 208 °C). ^1H NMR (CD_2Cl_2): δ 15.82 (brs, 1H, AcrH), 9.62 (s, 1H, AcrH), 8.65 (d, J = 8.9 Hz, 2H, AcrH), 8.38 (d, J = 8.5 Hz, 2H, AcrH), 8.27 (m, 2H, AcrH), 7.92 (m, 2H, AcrH), ^{19}F NMR (CD_2Cl_2): δ –78.94 (s, $CF_3SO_3^-$).$^{13}C\{^1H\}$ NMR (CD_2Cl_2): δ 148.5, 140.4, 138.4, 129.7, 128.8, 126.5, 121.0 (q, $^1J_{C\text{-}F}$ = 319 Hz, $CF_3SO_3^-$), 120.8. Anal. Calc. For $C_{14}H_{10}F_3NO_3S$ (329.29): C, 51.06; H, 3.06; N, 4.25. Found: C, 51.18; H, 2.96; N, 4.27%. Main IR bands (ν, cm^{-1}): 3090, 3048, 3011, 2916, 2888, 2837, 2777, 1647, 1626, 1587, 1481, 1464, 1425, 1401, 1284, 1221, 1156, 1026, 776, 742, 674, 632, 601, 572, 515.

2.3. Isolation of $\{([C_{13}H_{10}N][CF_3SO_3])_2{\cdot}C_{14}H_{10}\}$ (4)

Three molar equivalents of anthracene ($C_{14}H_{10}$, *Acros*, 99% purity) (0.466 g, 2.607 mmol) and acridine ($C_{13}H_9N$, *Acros*, 98% purity) (0.467 g, 2.607 mmol) were successively added to a colourless solution of [*n*-$Bu_2Sn(OH)(H_2O)(CF_3SO_3)]_2$ (**1**) (0.709 g, 0.869 mmol) in dichloromethane (25 mL) at room temperature. After stirring for two hours, fresh toluene (15 mL), used as co-solvent for crystallization, was then introduced to the resulting dark red solution. After few days at room temperature, colourless square single-crystals were first obtained, corresponding to organotin(IV) complex **5a**. After separation, dark red square single crystals were grown from the mother liquor by slow evaporation. The crystals were filtered off, washed with portions of *n*-pentane, dried in air at room temperature, and finally characterized as salt $\{([C_{13}H_{10}N][CF_3SO_3])_2{\cdot}C_{14}H_{10}\}$ **4** (mp 178 °C). ^1H NMR (CD_2Cl_2): δ 15.88 (brs, 2H, AcrH), 9.59 (s, 2H, AcrH), 8.69 (d, J = 8.9 Hz, 4H, AcrH), 8.47 (s, 2H, Ant), 8.37 (d, J = 8.5 Hz, 4H, AcrH), 8.29 (m, 4H, AcrH), 8.05 (m, 4H, Ant), 7.94 (m, 4H, AcrH), 7.50 (m, 4H, Ant). ^{19}F NMR (CD_2Cl_2): δ –78.94 (s, $CF_3SO_3^-$). $^{13}C\{^1H\}$ NMR (CD_2Cl_2): δ 148.5 (AcrH), 140.4 (AcrH), 138.4 (AcrH), 132.0 (Ant), 129.7 (AcrH), 128.8 (AcrH), 128.4 (Ant), 126.5 (AcrH), 126.4 (Ant), 125.7 (Ant), 121.0 (q, $^1J_{C\text{-}F}$ = 319 Hz, $CF_3SO_3^-$), 120.7 (AcrH). Anal. Calc. For $C_{42}H_{30}F_6N_2O_6S_2$ (836.82): C, 60.28; H, 3.61; N, 3.35. Found: C, 59.90; H, 3.16; N, 3.52%. Main IR bands (ν, cm^{-1}): 3302, 3257, 3208, 3148, 3103, 3059, 3024, 2989, 2948, 2872, 1650, 1476, 1427, 1257, 1224, 1154, 1028, 873, 790, 757, 727, 618, 574, 516.

2.4. X-Ray diffraction analysis

Diffraction data were collected from suitable crystals on a Bruker Nonius ApexII CCD (Mo Kα radiation, λ = 0.71073 Å). The structures were solved using Charge Flipping Algorithm Methods (SUPERFLIP) [12] and refined with full-matrix least-squares methods based on F^2 (SHELX-97) [13] with the aid of the WINGX program [14]. All non-hydrogen atoms were refined with anisotropic thermal parameters and hydrogen atoms were included in their calculated positions and refined with a

Table 1
Crystal and structure refinement data for **2**, **3** and **4**.

Compounds	**2**	**3**	**4**
Empirical formula	$C_{13}H_{10}N{\cdot}H_2O$, CF_3SO_3	$C_{13}H_{10}N$, CF_3SO_3	$C_{13}H_{10}N{\cdot}0.5\ C_{14}H_{10}$, CF_3SO_3
Formula weight (g.mol^{-1})	347.31	329.29	418.40
Temperature (K)	115(2)	115(2)	115(2)
Crystal system	Orthorhombic	Triclinic	Triclinic
Space group	*Pnma*	$P\bar{1}$	$P\bar{1}$
a (Å)	11.6289(7)	7.0899(3)	9.0072(4)
b (Å)	6.6998(5)	9.6716(4)	10.1453(4)
c (Å)	18.6130(11)	10.5407(4)	11.2361(5)
α (°)		74.269(2)	69.110(2)
β (°)		78.855(2)	81.158(2)
γ (°)		81.869(2)	69.894(2)
Volume (Å^3)	1450.16(16)	679.55(5)	900.24(7)
Z	4	2	2
ρ_{calc} (g.cm^{-3})	1.591	1.609	1.544
μ (mm^{-1})	0.277	0.286	0.234
F(000)	712	336	430
Crystal size (mm^3)	0.25 × 0.05 × 0.05	0.22 × 0.13 × 0.10	0.42 × 0.08 × 0.04
sin(θ)/λ max (Å^{-1})	0.65	0.65	0.65
Index ranges	*h*: −14; 9	*h*: −9; 9	*h*: −11; 11
	k: −7; 8	*k*: −12; 12	*k*: −13; 13
	l: −22; 24	*l*: −13; 12	*l*: −14; 14
Reflections collected	5343	5501	12073
R_{int}	0.0502	0.0159	0.0582
Reflections with $I \geq 2\sigma(I)$	1360	2852	3466
Data/restraints/parameters	1740/0/133	3074/0/199	4074/0/262
Final *R* indices [$I \geq 2\sigma(I)$]	$R1$[a] = 0.0487	$R1$[a] = 0.0388	$R1$[a] = 0.0471
	$wR2$[b] = 0.0911	$wR2$[b] = 0.0995	$wR2$[b] = 0.1016
R indices (all data)	$R1$[a] = 0.0703	$R1$[a] = 0.0420	$R1$[a] = 0.0581
	$wR2$[b] = 0.1013	$wR2$[b] = 0.1018	$wR2$[b] = 0.1085
Goodness-of-fit[c] on F^2	1.143	1.104	1.062
Largest difference peak and hole (e Å^{-3})	0.307 and −0.320	0.407 and −0.310	0.348 and −0.462
CCDC deposition no.	891927	891928	891929

[a] $R1 = \Sigma(||F_o|-|F_c||)/\Sigma|F_o|$.

[b] $wR2 = [\Sigma w(F_o^2-F_c^2)^2/\Sigma[w(F_o^2)^2]^{1/2}$ where $w = 1/[\sigma^2(Fo^2 + (0.0107P)^2 + 1.9231P]$ for **2**, $w = 1/[\sigma^2(Fo^2 + (0.0347P)^2 + 0.5841P]$ for **3**, $w = 1/[\sigma^2(Fo^2 + (0.0253P)^2 + 1.0201P]$ for **4**, where $P = (\mathrm{Max}(Fo^2.0) + 2Fc^2)/3$.

[c] $S = [\Sigma w(F_o^2-F_c^2)^2/(n-p)]^{1/2}$ (n = number of reflections, p = number of parameters).

riding model. Programs used for the representation of the molecular and crystal structures: ORTEP [15], DIAMOND [16], and MERCURY [17]. Crystallographic data and structures refinement details or **2**, **3** and **4** are summarized in Table 1.

Crystallographic data for the structures reported in this paper have been deposited at the Cambridge Crystallographic Data Centre, CCDC, No. CCDC 891927 for **2**, No. CCDC 891928 for **3**, and No. CCDC 891929 for **4**. Copies of the data may be obtained free of charge from the Director, CCDC, 12 Union Road, Cambridge CB2 1EZ, UK (fax: int Code +44 1223 336 033; e-mail: deposit@ccdc.cam.ac.uk or http://www.ccdc.cam.ac.uk).

3. Results and discussion

Synthetic pathways of compounds **2**-**4** are summarized in Scheme 2.

3.1. Isolation and crystal structures of acridinium salts 2 and 3

The strategy recently developed for the design of phenazinium-based stacks [4b,11] was applied to acridine. Thus, the reaction of the dimeric hydroxo di-*n*-butylstannane trifluoromethanesulfonato complex [*n*-$Bu_2Sn(\mu$-OH)$(H_2O)(^1$-$O_3SCF_3)]_2$ (**1**) with acridine ($C_{13}H_9N$, Acr) (1:3 molar ratio) in dichloromethane at room temperature led to colourless crystals of the tetra-*n*-butyldistannoxane trifluoromethanesulfonato cluster (**5**). Compound **5** could be isolated in two polymorphic forms **5a** and **5b** which crystallized in two distinct crystal systems (triclinic-$P\bar{1}$ and monoclinic-$P2_1/n$, respectively), and with specific crystal habits (square and rod) that easily facilitate their visual identification [4b]. According to the infrared fingerprints recorded on crystals, and which are also characteristic for each polymorph (shown in the Supporting Information, Fig. S1), we can unambiguously conclude that both structures of **5** are formed successively during the reaction. Moreover, the monitoring of the reaction by $^{119}Sn\{^1H\}$ spectroscopy showed, after addition of three molar equivalents of acridine to a CD_2Cl_2 solution of **1**, the predominant formation of the pair of the characteristic resonances of the distannoxane species **5a** at δ = −135 and −143 ppm (Fig. S2). Upon crystallization of **5a** and **5b**, and separation by filtration, two new types of yellow crystals were grown together from the mother liquor. They were collected as needles and plates, and were identified as the acridinium

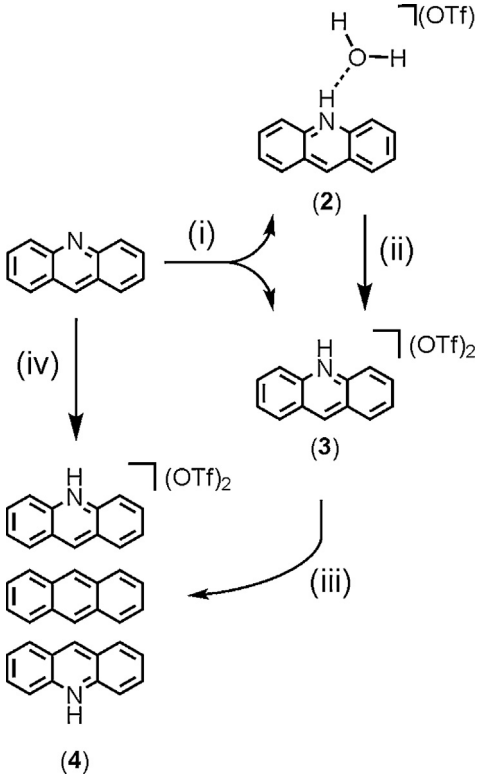

Scheme 2. Reagents and conditions: (i) Complex **1**, CH_2Cl_2, room temperature (RT), crystallisation from CH_2Cl_2/toluene; (ii) a) molecular sieves, CH_2Cl_2/toluene, b) solventless conditions, 100 °C, under vacuum; (iii) Ant, CH_2Cl_2/toluene, RT; (iv) Ant, complex **1**, CH_2Cl_2, RT, crystallisation from CH_2Cl_2/toluene.

trifluoromethanesulfonate salts $[C_{13}H_{10}N]^+[CF_3SO_3]^-$, **2** and **3**, respectively. From a mechanistic point of view, the removal of protons from **1** by acridine molecules leads to the in situ formation of acridinium cations (AcrH), and promotes the rearrangement of organotin species into tetranuclear oxo-cluster **5**. This subsequently led to the release of $CF_3SO_3^-$, which ultimately compensates the positive charge of AcrH.

The difference between the acridinium salts **2** and **3** comes exclusively from the presence of a water molecule in the crystal lattice of one of the two salts. Indeed, the infrared spectrum recorded from **2** exhibits the characteristic vibration bands of the trifluoromethasulfonate anions (in the stretching region between 1000 and 1300 cm^{-1} [18], and also observed for **3**), and a broad elongation band at 3387 cm^{-1}. This band is a strong evidence of the presence of water. It is not present in the spectrum of **3**. It can be attributed to the σ(OH) vibration. The ^1H NMR spectra of **2** and **3** corroborate this observation (IR and NMR spectra are shown in the Supporting Information). The X-ray crystallographic analysis of **2** confirms the hydrogen bond occurring between the NH group of the acridium cation (AcrH) and one molecule of water [N(H)···O = 2.680(3) Å and 179.4°]. The acridinium and water molecules are located in the same mirror plane. Furthermore, the water molecule is also in hydrogen bonding interaction with one oxygen atom of the

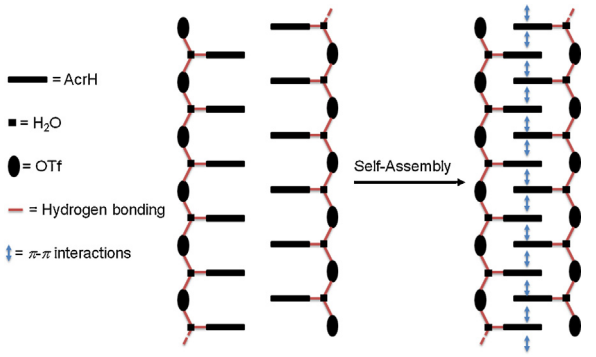

Scheme 3. Schematic representation of the supramolecular construction of **2**.

trifluoromethanesulfonate anion [O(H)···O = 2.755(2) Å and 177.3°]. An ORTEP view of **2** is shown in Fig. 1a together with selected bond distances and angles. Interestingly, and from a supramolecular point of view, the water molecule in each $[C_{13}H_{10}N{\cdot}H_2O][CF_3SO_3]$ unit is also implicated in a third hydrogen-bonding interaction, with an identical distance that previously [O(H)···O = 2.755(2) Å], with an oxygen atom of an adjacent trifluoromethanesulfonate anion, leading to the formation of an one-dimensional infinite polymer chain propagating along the *b* axis, and which consists of $H_2O\cdots CF_3SO_3$ building blocks as repeating unit. The AcrH cations are orthogonally positioned along this chain, parallel to plane (010) and in an isotactic arrangement. As a result of the self-assembly induced by π-π interactions between anti-parallel acridinium rings, two polymeric chains are fitted into each other. It leads to a 2-D architecture which can be compared to a ladder structure. The construction of the resulting supramolecular edifice is summarized in Scheme 3 and a view of the crystal packing is shown in Fig. 1b. The interplanar and the centroid-to-centroid distances between parallel AcrH are 3.35 and 4.35 Å, respectively. The difference in these two distances indicates that acridinium rings are strongly slipped. The slip angle (angle between the normal to the planes and the centroid–centroid vector) is 39.75°, corresponding to a slippage distance of 2.79 Å. Typically for such interactions, the interplanar distance between the arene planes is commonly found around 3.3 to 3.8 Å [19]. Interestingly, the organization of the crystal packing described for **2** is comparable to ionic supramolecular architectures reported in the past by Wolf and Mei, and prepared from acridine and dicarboxylic acids [20].

Salt **3** corresponds to the dehydrated form of **2**. Initially, both salts crystallized together from the same batch but they are only distinguished by their respective shape (needles for **2** and plates for **3**). However, the conversion of **2** into **3** occurs when molecular sieves were added to a dichloromethane solution of **2** or alternatively when **2** is heated at the solid state under vacuum at 100 °C for 1 hour (Scheme 2, pathway (ii)). On the basis on an X-ray crystallographic analysis, the molecular structure of **3** can be described as constituted by an acridium cation, AcrH $[C_{13}H_{10}N]^+$, and by a trifluoromethanesulfonate

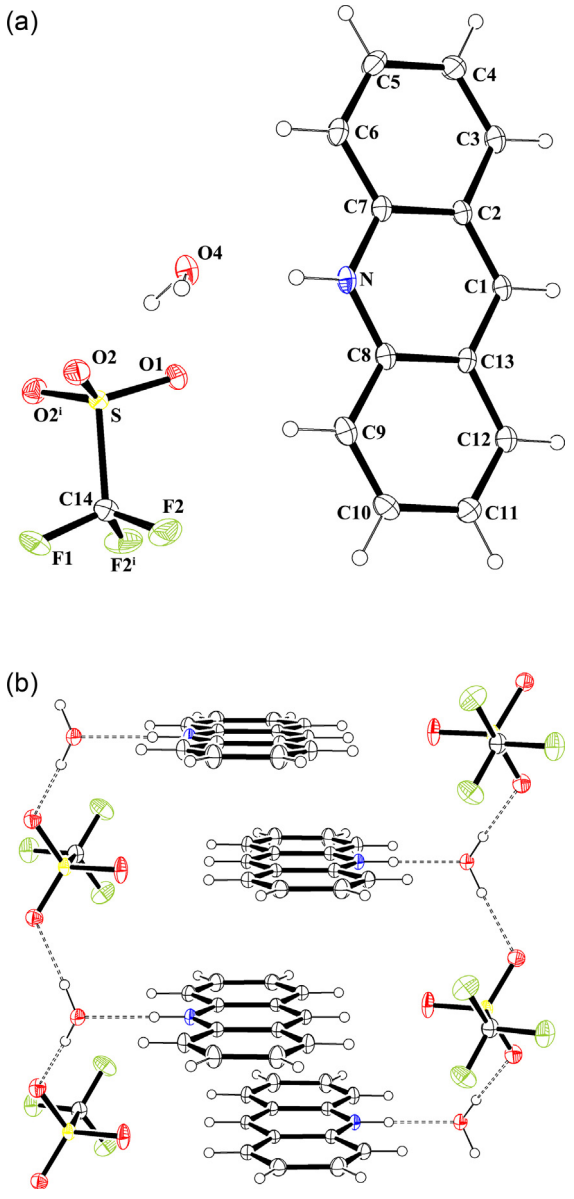

Fig. 1. a: molecular structure of $[C_{13}H_{10}N{\cdot}H_2O][CF_3SO_3]$ (**2**) showing the atom labelling scheme (ORTEP view). Colour code: sulphur: yellow; oxygen: red; nitrogen: blue; fluoride: green; carbon: grey; hydrogen: white (online). Selected bond lengths (A) and angles (°): N–C7 1.350(4), N–C8 1.360(4), C1–C2 1.388(4), C1–C13 1.393(4), C2–C3 1.421(5), C2–C7 1.427(4), C3–C4 1.359(5), C4–C5 1.417(5), C5–C6 1.360(5), C6–C7 1.409(5), C8–C9 1.408(5), C8–C13 1.426(4), C9–C10 1.360(5), C10–C11 1.432(5), C11–C12 1.353(5), C12–C13 1.425(5), S–O1 1.435(2), S–O2 1.445(2), S–C14 1.825(4), F1–C14 1.327(4), F2–C14 1.323(3); C7–N–C8 123.6(2), C2–C1–C13 121.1(2), C1–C2–C3 123.3(3), C1–C2–C7 118.7(3), C3–C2–C7 118.0(3), C4–C3–C2 120.7(3), C3–C4–C5 120.3(3), C6–C5–C4 121.3(3), C5–C6–C7 119.3(3), N–C7–C6 120.6(3), N–C7–C2 119.0(3), C6–C7–C2 120.4(3), N–C8–C9 120.9(3), N–C8–C13 118.8(3), C9–C8–C13 120.4(3), C10–C9–C8 119.5(3), C12–C11–C10 120.3(3), C11–C12–C13 120.5(3), C1–C13–C12 123.0(3), C1–C13–C8 118.7(3), C12–C13–C8 118.3(3), O1–S–O2 115.39(9), O1–S–C14 103.67(16), O2–S–C14 103.17(10), F2–C14–F1 108.0(2), F2–C14–S 111.05(18), F1–C14–S 110.6(2). Symmetry transformations used to generate equivalent atoms (^{i}): $x,-y+3/2,z$; b: the crystal packing of **2** in the unit cell (DIAMOND representation). Hydrogen bonding interactions [N(H)···O and O(H)···O] are shown by dashed lines. Colour code: sulphur: yellow; oxygen: red; nitrogen: blue; fluoride: green; carbon: grey; hydrogen: white (online).

anion $[CF_3SO_3]^-$ in hydrogen bonding interaction with the NH group of the cation [N(H)···O = 2.743(2) Å and 169.34°]. An ORTEP representation of **3** is shown in Fig. 2a.

From a supramolecular point of view, acridinium rings of **3** are self-assembled in antiparallel arrangement along the *a*-axis, and through π-π interactions leading to columnar oblique stacks in which the rings emerge tilted by 22.6° with respect to the (100) plane. Two values of interplanar distances, alternating, have been determined between AcrH: 3.218 Å [centroid-to-centroid distance = 4.584 Å, implicating a slippage of 3.26 Å (slip angle 45.35°)] and 3.349 Å [centroid-to-centroid distance = 3.698 Å, implicating a slippage of 1.56 Å (slip angle 25.03°)]. Additionally, short intramolecular contacts exist also between fluorine and oxygen atoms of trifluoromethanesulfonate anions and the nearest neighbour molecules of acridinium, through O···(H)C and F···(H)C interactions, and thus uniting the columns, to each others. A short F···F distance (2.910(2) Å), slightly lower than the sums of the van der Waals radii (2.94), is also observed. A view of the crystal packing of **3** in the unit cell is reported in Fig. 2b.

3.2. Isolation and crystal structures of acridinium salt 4

In previous studies, we reported the incorporation of neutral polyaromatic molecules, e.g. phenazine and anthracene, between two phenazinium salts, leading to unusual sandwich-type structures [4b,11]. A similar methodology was used in the case of acridine. When an equimolar mixture of acridine and anthracene reacts with organotin(IV) complex **1**, nice red-blood square crystals were grown in addition to colourless crystals corresponding to organotin(IV) cluster **5**. The X-ray crystallographic analysis performed on suitable red crystals, indeed, revealed the expected sandwich-type structure and determined as $\{([C_{13}H_{10}N][CF_3SO_3])_2{\cdot}C_{14}H_{10}\}$ (**4**) resulting from the intercalation of a neutral molecule of anthracene between two acridiniunium trifluoromethanesulfonate salt molecules via slipped parallel π-π aromatic interactions. The micro-analytical data corroborates the formulation reported for **4**. The average inter-planar distance between the aromatic rings is 3.424 Å. The two rings are slipped by 1.52 Å (slip angle equal to 23.90°) and the ring-centroid to ring-centroid distances are equal to 3.74 Å. One of the oxygen atoms of the trifluoromethanesulfonate anion is engaged in an intermolecular hydrogen bonding interaction with the NH function of the acridinium cation [N–H···O = 2.774(3) Å and 169.06°]. As in the case of **3**, additional short intramolecular contacts are observed between fluorine and oxygen atoms of trifluoromethanesulfonate anions and surrounding molecules of anthracene or acridinium, through O···(H)C and F···(H)C interactions. An ORTEP representation and the crystal packing of salt **4** are reported in Fig. 3a and b, respectively.

Furthermore, the π-π stacking occurring between the acridinium and anthracene rings brings the CF_3 groups of trifluoromethanesulfonate anions in close proximity, in a face-to-face orientation. The resulting F···F distance (2.892(2) Å), shorter than that observed in the crystal packing of **3**, can be described as a type I conformation

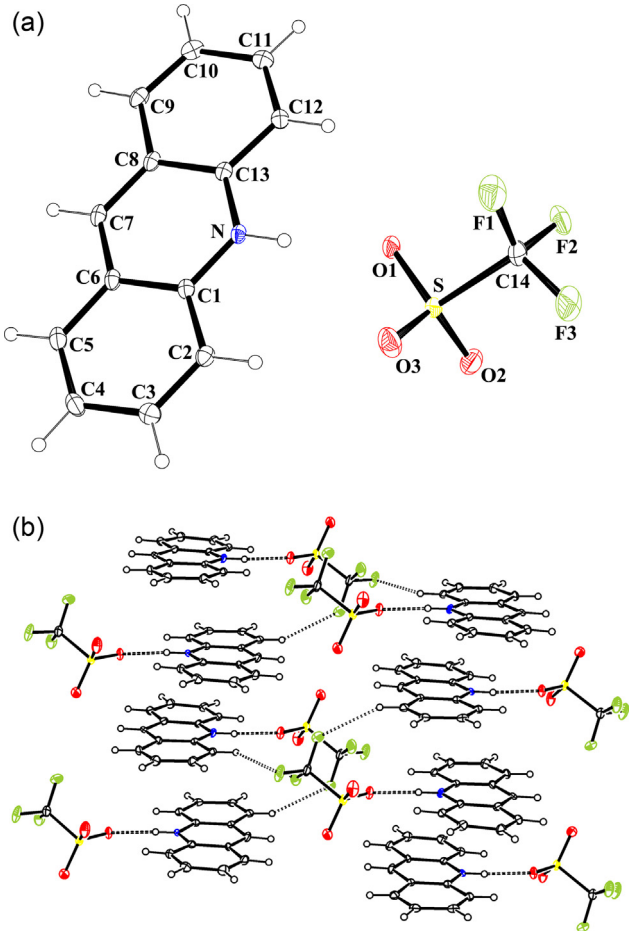

Fig. 2. a: molecular structure of $[C_{13}H_{10}N][CF_3SO_3]$ (**3**) showing the atom labelling scheme (ORTEP view). Colour code: sulphur: yellow; oxygen: red; nitrogen: blue; fluoride: green; carbon: grey; hydrogen: white (online). Selected bond lengths (A) and angles (°): C1–N 1.359(2), C1–C2 1.411(2), C1–C6 1.427(2), C2–C3 1.366(2), C3–C4 1.418(2), C4–C5 1.361(3), C5–C6 1.430(2), C6–C7 1.395(2), C7–C8 1.397(2), C8–C13 1.426(2), C8–C9 1.430(2), C9–C10 1.357(3), C10–C11 1.423(2), C11–C12 1.368(2), C12–C13 1.415(2), C13–N 1.355(2), C14–F1 1.323(2), C14–F3 1.330(2), C14–F2 1.332(2), C14–S 1.8249(18), S–O2 1.4357(14), S–O3 1.4389(14), S–O1 1.4511(12); N–C1–C2 120.28(14), N–C1–C6 118.89(14), C2–C1–C6 120.83(15), C3–C2–C1 118.85(15), C2–C3–C4 121.36(16), C5–C4–C3 120.77(16), C4–C5–C6 120.03(15), C7–C6–C1 118.53(15), C7–C6–C5 123.34(15), C1–C6–C5 118.13(15), C6–C7–C8 121.28(14), C7–C8–C13 118.58(15), C7–C8–C9 123.48(14), C13–C8–C9 117.95(15), N–C13–C12 120.06(14), N–C13–C8 118.94(14), C13–N–C1 123.75(13), F1–C14–F3 108.84(16), F1–C14–F2 107.52(16), F3–C14–F2 107.05(14), F1–C14–S 111.56(12), F3–C14–S 110.92(13), F2–C14–S 110.77(13), O2–S–O3 115.58(10), O2–S–O1 114.43(9), O3–S–O1 113.78(8), O2–S–C14 103.84(8), O3–S–C14 104.06(9), O1–S–C14 103.10(8); b: the crystal packing of **3** in the unit cell (DIAMOND representation). Hydrogen bonding interactions [N(H)···O] and [C(H)···F] are shown by dashed lines. Colour code: sulphur: yellow; oxygen: red; nitrogen: blue; fluoride: green; carbon: grey; hydrogen: white (online).

according to the Desiraju's classification (C–F···F = 95.58 and 120.95°, angle dihedral 74°) [21,22]. Two fluorine atoms of each trifluoromethanesulfonate anions are involved in such an interaction. A MERCURY representation focusing on this contact is depicted in Fig. 4. Synthetically, the sandwich structure of **4** can be also obtained mixing two equivalents of **3** with one equivalent of anthracene in dichloromethane solution (Scheme 2, pathway (iii)).

Thus, the three types of supramolecular stacks described in this study and built from acridinium trifluoromethanesulfonates result from the simultaneous

Table 2
π-π stacking parameters for **2**, **3** and **4**.

Compound direction	Interplanar distance (Å)	Centroïd to centroïd distance (Å)	Slip angle (°)	Slippage distance (Å)	Direction
2	3.35	4.35	39.75	2.79	*b*
3	3.22	4.58	45.35	3.26	*a*
	3.35	3.70	25.03	1.56	*a*
4	3.42	3.74	23.90	1.52	*c*

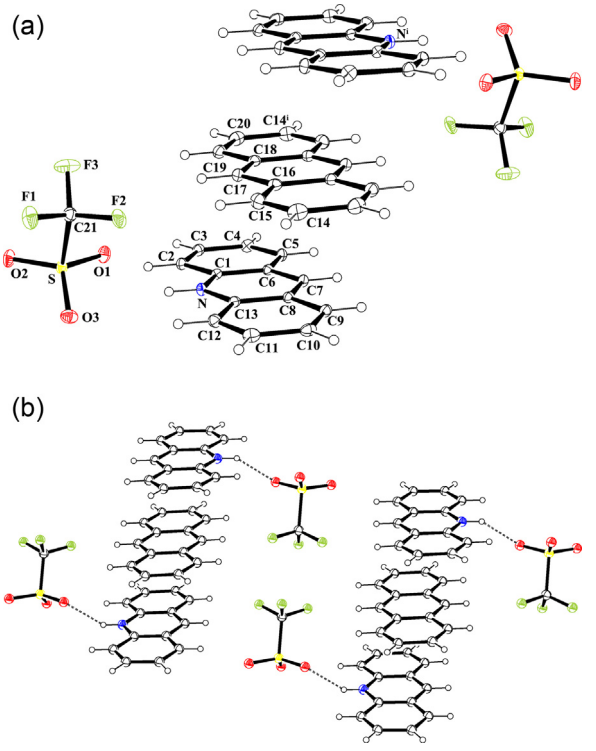

Fig. 3. a: molecular structure of $\{([C_{13}H_{10}N][CF_3SO_3])_2{\cdot}C_{14}H_{10}\}$ (**4**) showing the atom labelling scheme (ORTEP view). Colour code: sulphur: yellow; oxygen: red; nitrogen: blue; fluoride: green; carbon: grey; hydrogen: white (online). Selected bond lengths (A) and angles (°): C1–C6 1.369(3), C1–C2 1.421(3), C2–C3 1.366(3), C3–C4 1.428(3), C4–C7 1.395(3), C4–C5 1.422(3), C5–N 1.354(2), C5–C6 1.420(3), C7–C8 1.393(3), C8–C9 1.425(3), C8–C11 1.429(3), C9–N 1.354(2), C9–C14 1.415(3), C11–C12 1.361(3), C12–C13 1.418(3), C13–C14 1.365(3), C15–C16 1.362(3), C16–C17 1.430(3), C17–C18 1.393(3), C18–C19 1.398(3), C19–C20 1.430(3), C20–C21 1.361(3), C21–F3 1.324(2), C21–F2 1.336(2), C21–F1 1.340(2), C21–S 1.826(2), O1–S 1.4472(16), O2–S 1.4429(16), O3–S 1.4386(16); C6–C1–C2 121.79(18), C3–C2–C1 120.40(18), C2–C3–C4 120.05(17), C7–C4–C5 118.87(17), C7–C4–C3 122.61(17), C5–C4–C3 118.52(17), N–C5–C6 120.38(17), N–C5–C4 118.73(17), C6–C5–C4 120.89(17), C1–C6–C5 118.35(17), C8–C7–C4 121.17(17), C7–C8–C9 118.32(17), C7–C8–C11 123.29(17), C9–C8–C11 118.39(18), N–C9–C14 120.30(17), N–C9–C8 119.19(17), C14–C9–C8 120.50(18), C9–N–C5 123.71(16), C12–C11–C8 120.20(18), C11–C12–C13 120.35(19), C14–C13–C12 121.72(19), C13–C14–C9 118.82(18), C15–C16–C17 120.7(2), C18–C17–C16 122.22(18), C17–C18–C19 121.59(18), C18–C19–C20 122.25(19), C21–C20–C19 121.0(2), F3–C21–F2 107.90(17), F3–C21–F1 107.89(18), F2–C21–F1 106.59(16), F3–C21–S 111.89(14), F2–C21–S 110.90(14), F1–C21–S 111.45(14), O3–S–O2 115.64(10), O3–S–O1 114.73(10), O2–S–O1 115.14(9), O3–S–C21 103.02(9), O2–S–C21 103.64(9), O1–S–C21 102.00(9). Symmetry transformations used to generate equivalent atoms (^{i}): $-x+2,-y+2,-z$; b: the crystal packing of **4** in the unit cell (DIAMOND representation). Hydrogen bonding interactions [N(H)···O] are shown by dashed lines. Colour code: sulphur: yellow; oxygen: red; nitrogen: blue; fluoride: green; carbon: grey; hydrogen: white (online).

involvement of different types of intermolecular interactions: π-π aromatic interactions, hydrogen bonds that can be qualified as *strong* and *weak* [23], and also F···F contacts. All modes of interaction which are implicated in the crystal packing of **2**, **3** and **4** are listed in Tables 2 and 3. In the three architectures, acridinium cations are directly involved in π-π aromatic stacking and in *strong* hydrogen bond interactions (N–H···O), with water molecules (**2**) or

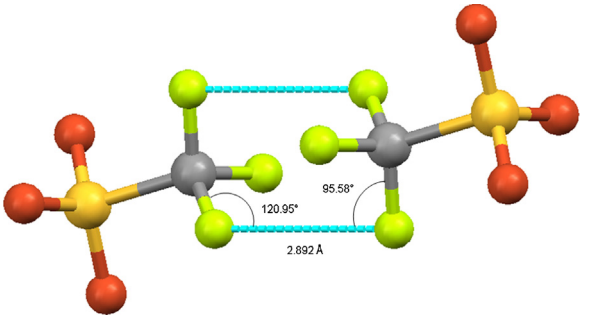

Fig. 4. F···F interactions (dashed lines) involving the CF_3 groups of the trifluoromethanesulfonate anions of **4** (MERCURY representation). Colour code: sulphur: yellow; oxygen: red; fluoride: green; carbon: grey.

Table 3
Geometry of hydrogen bonds and short contacts for **2**, **3** and **4**.

Compound	Interaction	D[a]-H (Å)	H···A[b] (Å)	D···A (Å)	D-H···A (°)	Direction
2	N–H···O	0.86	1.82	2.68	179	*c*
	O–H···O	0.87	1.88	2.75	177	*b*
	C–H···O	0.93	2.44	3.28	149	*c*
	C–H···O	0.93	2.49	3.30	146	*c*
	C–H···F	0.93	2.52	3.20	130	*a*
3[c]	N–H···O	0.86	1.89	2.74	170	*c*
	C–H···O	0.93	2.50	3.34	149	*c*
	C–H···O	0.93	2.50	3.41	165	*c*
	C–H···O	0.93	2.63	3.20	120	*b*
	C–H···F	0.93	2.60	3.47	155	*c*
	C–H···F	0.93	2.64	3.48	150	*c*
4[c]	N–H···O	0.86	2.02	2.77	146	*a*
	N–H···O	0.86	2.60	3.08	117	*c*
	C–H···O	0.93	2.63	3.50	157	*a*
	C–H···O	0.93	2.48	3.26	141	*a*
	C–H···O	0.93	2.69	3.61	169	*a*
	C–H···O	0.93	2.59	3.45	153	*b*
	C–H···O	0.93	2.52	3.19	130	*a*
	C–H···F	0.93	2.52	3.40	159	*b*

[a] Hydrogen bond donor.
[b] Hydrogen bond acceptor.
[c] In addition to these intermolecular interactions, the crystal packing of **3** and **4** exhibits also short F···F contacts occurring between $CF_3SO_3^-$ anions.

$F_3CSO_3^-$ anions (**3** and **4**). According to us, these interactions can be considered as the main driving forces leading to the reported self-assembled edifices. In addition, the trifluoromethanesulfonates anions through their fluorine atoms and their oxygen atoms non implicated in *strong* intermolecular interactions strengthen the cohesion of the crystal packing building *bridges* between aromatic stacks *via* the formation of secondary (*weak*) C–H···O and C–H···F hydrogen bonding interactions and short F···F contacts. However, these weaker interactions can be also considered, owing to their orientation, as one of the factors responsible for the slippage, more or less marked (2.79 Å for **2**, 1.52 Å for **4**), observed between the acridinium rings in π-π interaction.

4. Conclusion

So far, the main crystal engineering strategy employed for the synthesis of supramolecular co-crystalline materi-

als based on acridine and phenazine synthons has required the use of suitable hydrogen bond donors as co-reactant. Thus, several examples have been previously reported in the literature describing the co-crystallisation of acridine or phenazine with 2,2′-dihydroxybiphenyl [24], 5,10-dihydrophenazine [25], dicarboxylic acids [20], 2,5-dibromo-3,6-dihydroxy-1,4-benzoquinone [26], hydroxyquinone and 1,5-dihydroxynaphthalene [27], *N*,*N*′-bis(2-pyridyl)aryldiamines [28], phloroglucinol [29], vanillin [30]. The resulting solid-state architectures have underlined the predisposition of such N-heterocyclic molecules to generate π-π stacking and hydrogen bonding interactions. In this paper, we have shown that the *supramolecular synthon* [31], in our case the acridinium trifluoromethanesulfonate, can be generated in situ in the presence of an organotin complex. To our knowledge, this approach involving an organometallic complex is innovative in the domain of crystal engineering. Further studies are in progress in our laboratory to extend the reported reaction for the construction of new π-π self-assembled molecular stacks.

Acknowledgements

Financial support from the Centre National de la Recherche Scientifique (CNRS, France) is gratefully acknowledged. The authors thank also Prof. Enrique Espinosa for his clarification on halogen···halogen interactions, Dr. Philippe Richard for his consideration of the structural part and Dr. Richard Decréau for the correction of the manuscript.

Appendix A. Supplementary data

Supplementary information for this article containing the FT-IR (ATR) spectra of polymorphic forms of **5** (Fig. S1), ^{119}Sn{^{1}H} NMR spectra of **1** and after addition of acridine (Fig. S2), FT-IR (ATR) spectra of **2** and **3** (Fig. S3), and ^{1}H, ^{19}F, and ^{13}C{^{1}H} NMR spectra of **2**, **3** and **4** (Fig. S4-S12) is available with the online version at http://dx.doi.org/10.1016/j.crci.2012.12.006.

References

[1] J. Beckmann, Appl. Organomet. Chem. 19 (2005) 494.
[2] (a) K. Sakamoto, H. Ikeda, H. Akashi, T. Fukuyama, A. Orita, J. Otera, Organometallics 19 (2000) 3242;
(b) A. Orita, J. Xiang, K. Sakamoto, J. Otera, J. Organomet. Chem. 624 (2001) 287.
[3] D. Ballivet-Tkatchenko, H. Cattey, L. Plasseraud, P. Richard, Acta Crystallogr. E62 (2006) m2820.
[4] (a) P.B. Hitchcock, M.F. Lappert, G.A. Lawless, G.M. de Lima, L.J.M. Pierssens, J. Organomet. Chem. 601 (2000) 142;
(b) L. Plasseraud, H. Cattey, P. Richard, D. Ballivet-Tkatchenko, J. Organomet. Chem. 694 (2009) 2386.
[5] T. Sato, Y. Wakahara, J. Otera, H. Nozaki, Tetrahedron 47 (1991) 9773.
[6] T. Sato, Y. Wakahara, J. Otera, H. Nozaki, Tetrahedron Lett. 31 (1990) 1581.
[7] K. Sakamoto, Y. Hamada, H. Akashi, A. Orita, J. Otera, Organometallics 18 (1999) 3555.
[8] H. Lee, J.Y. Bae, O.S. Kwon, S.J. Kim, S.D. Lee, H.S. Kim, J. Organomet. Chem. 689 (2004) 1816.
[9] P. Švec, R. Olejník, Z. Padělková, A. Růžička, L. Plasseraud, J. Organomet. Chem. 82 (2012) 708.
[10] (a) D. Ballivet-Tkatchenko, T. Jerphagnon, R. Ligabue, L. Plasseraud, D. Poinsot, Appl. Catal. A: Gen. 255 (2003) 93;
(b) D. Ballivet-Tkatchenko, R. Burgat, S. Chambrey, L. Plasseraud, P. Richard, J. Organomet. Chem. 691 (2006) 1498;
(c) D. Ballivet-Tkatchenko, S. Chambrey, R. Keiski, R. Ligabue, L. Plasseraud, P. Richard, H. Turunen, Catal. Today 115 (2006) 80;
(d) D. Ballivet-Tkatchenko, H. Chermette, L. Plasseraud, O. Walter, Dalton Trans. (2006) 5167;
(e) L. Plasseraud, H. Cattey, P. Richard, 64b, Z. Naturforsch (2009) 831;
(f) L. Plasseraud, D. Ballivet-Tkatchenko, H. Cattey, S. Chambrey, R. Ligabue, P. Richard, R. Willem, M. Biesemans, J. Organomet. Chem. 695 (2010) 1618;
(g) G. Laurenczy, M. Picquet, L. Plasseraud, J. Organomet. Chem. 696 (2011) 1904;
(h) D. Ballivet-Tkatchenko, F. Bernard, F. Demoisson, L. Plasseraud, S.R. Sanapureddy, Chem. Sus. Chem. 4 (2011) 1316.
[11] L. Plasseraud, B. Therrien, A. Ruzicka, H. Cattey, Inorg. Chem. 380 (2012) 50.
[12] L. Palatinus, G. Chapuis, J. Appl. Cryst. 40 (2007) 786.
[13] G.M. Sheldrick, Shelx-97 (Includes Shelxs-97 and Shelxl-97), Release 97-2, Programs for the Refinement of Crystal Structures, University of Göttingen, Göttingen (Germany) 1998.
[14] L.J. Farrugia, J. Appl. Crystallogr. 32 (1999) 837.
[15] C.K. Johnson, M.N. Burnett, Ortep-III, Rep. ORNL-6895, Oak Ridge National Laboratory, Oak Ridge, TN (USA) 1996. Windows version: L.J. Farrugia, University of Glasgow, Glasgow, Scotland (U.K.) 1999. See also: L.J. Farrugia, J. Appl. Crystallogr. 30 (1997) 565.
[16] K. Brandenburg, DIAMOND (version 3.1), Crystal and Molecular Structure Visualization Crystal Impact–K, Brandenburg & H. Putz GbR, Bonn (Germany), 2005.
[17] C.F. Macrae, I.J. Bruno, J.A. Chisholm, P.R. Edgington, P. McCabe, E. Pidcock, L. Rodriguez-Monge, R. Taylor, J. van de Streek, P.A. Wood, M ercury CSD 2.0 - new features for the visualization and investigation of crystal structures, J. Appl. Crystallorg. 41 (2008) 466.
[18] (a) G.A. Lawrance, Chem. Rev. 86 (1986) 17;
(b) D.H. Johnston, D.F. Shriver, Inorg. Chem. 32 (1993) 1045.
[19] (a) C. Janiak, J. Chem. Soc. Dalton Trans. (2000) 3885;
(b) J.G. Planas, C. Masalles, R. Sillanpää, R. Kivekäs, F. Teixidor, C. Viñas, Cryst. Eng. Comm. 8 (2006) 75.
[20] X. Mei, C. Wolf, Eur. J. Org. Chem. (2004) 4340.
[21] V.R. Pedireddi, D. Sherkhar Reddy, B. Satish Goud, D.C. Craig, A. David Rae, G.R. Desiraju, J. Chem. Soc. Perkin Trans. 2 (1994) 2353.
[22] K. Reichenbächer, H.I. Süss, J. Hulliger, Chem. Soc. Rev. 34 (2005) 22.
[23] (a) G.R. Desiraju, T. Steiner, The Weak Hydrogen Bond in Structural Chemistry and Biology, Oxford University Press, Oxford, 1999;
(b) G.R. Desiraju, Acc. Chem. Res 35 (2002) 565.
[24] T. Smolka, R. Boese, R. Sustmann, Struct. Chem. 10 (1999) 429.
[25] V.R. Thalladi, T. Smolka, A. Gehrke, R. Boese, R. Sustmann, New J. Chem. 24 (2000) 143.
[26] M. Tomura, Y. Yamashita, Cryst. Eng. Comm. 2 (2000) 92.
[27] V.R. Thalladi, T. Smolka, A. Gehrke, R. Boese, R. Sustmann, Cryst. Eng. Comm. 2 (2000) 96.
[28] M. Gdaniec, I. Bensemann, T. Poloński, Cryst. Eng. Comm. 7 (2005) 433.
[29] B. Sarma, L.S. Reddy, A. Nangia, Cryst. Growth. Des. 8 (2008) 4546.
[30] D. Braga, F. Grepioni, L. Maini, P.P. Mazzeo, K. Rubini, Thermochim. Acta 507–508 (2010) 1.
[31] G.R. Desiraju, Angew. Chem. Int. Ed. Engl. 34 (1995) 2311.